# Elastic Behavior of Woven Hybrid Composites

TAKASHI ISHIKAWA* AND TSU-WEI CHOU

*Mechanical and Aerospace Engineering Department*
*University of Delaware*
*Newark, Delaware 19711*

**ABSTRACT**

Basic geometrical and material parameters are identified to characterize the structure of hybrid fabrics. Analysis of the elastic behavior is made based upon a mosaic model and the fabric composite can be regarded as an assemblage of assymetrical crossply laminates. Upper and lower bounds of elastic properties have been obtained and the results compare very favorably with experiments. The influence of fabric parameters on the elastic behavior has been demonstrated especially for the bending-stretching coupling effect. Essential considerations for fabric design also have been discussed.

## INTRODUCTION

THE SCIENCE AND technology of woven fabrics are not new. However, the understanding of composite material reinforced with woven fabrics is still in its infancy. The intent of this paper is to investigate the elastic properties of composites reinforced with hybrid fabrics, where more than one type of fibers are used. The state-of-the-art of non-woven hybrid composites has been reviewed by Chou and Kelly [1]. Mechanical properties of unidirectional hybrid composites can be found in the recent work of Chou, Gruber, and Fukuda [2—4], and Ji, Hsiao and Chou [5]. In the following, the basic structures of woven fabrics are introduced, and the geometrical as well as material parameters of hybrid woven fabrics are defined. Elastic properties are then examined as functions of these parameters.

### Non-Hybrid Fabric Composite

Woven fabrics have gained increasing popularity in the fabrication of structural components utilizing fiber composites. Fabric prepregs are particularly suitable, as compared to unidirectional tapes, for parts with complex contours such as corrugated webs of composite spars. The load carrying capacity of fabric composite, however, is lower than that of unidirectional tapes with the same amount of fibers.

All woven fabrics are formed by interlacing two sets of threads: the set of

*On leave from National Aerospace Laboratory, 1880 Jindaiji, Chofu, Tokyo 182, Japan.

*J. COMPOSITE MATERIALS,* Vol. 16 (January 1982) p. 2

0021-9983/82/01 0002—18 $04.50/0

vertical threads is called the warp and the horizontal threads are known as the filling [6,7]. The structure of a woven fabric, containing only one type of fiber can be understood from the two-dimensional representation of Figure 1. The various types of weaves can be identified by the patterns of repeats in the warp and filling directions. Two geometrical quantities are necessary: a filling thread is interlaced with every $n_{wg}$-th warp thread, and a warp thread is interlaced with every $n_{fg}$-th filling thread. Here, the subscripts $f$ and $w$ denote the filling and warp threads, respectively and $g$ signifies a geometrical parameter. This paper is restricted to the case of $n_{wg} = n_{fg} = n_g$. Fabrics with $n_g \geqslant 4$ and that the interlaced regions are not connected are known as satin weaves. 8th harness satin weaves ($n_g = 8$) have excellent pliability. A cross-sectional view of a fabric showing the interlaced regions is also given in Figure 1.

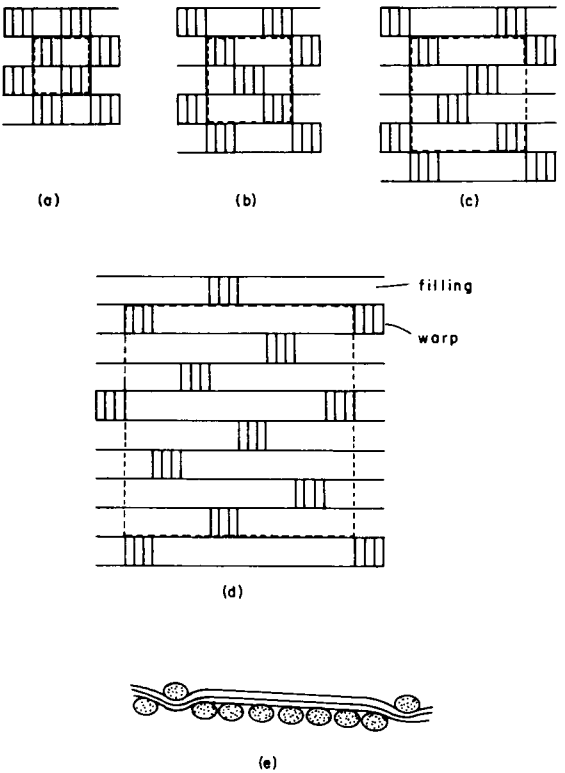


*Figure 1. Woven fabrics with several $n_g$ values. a) $n_g = 2$, plain weave, b) $n_g = 3$, twill weave, c) $n_g = 4$, 4th harness (crow foot) satin, d) $n_g = 8$, 8th harness satin, e) a cross-sectional view.*

### Hybrid Fabric Composite

Hybrid woven fabrics can offer a wide variety of fiber material selections for designers and significant improvements of the cost-effectiveness in fabrication [8]. In the analysis of this paper the bound approach [9] for non-hybrid fabric composites has been extended to hybrids. A basic difference between hybrid and non-hybrid fabric composites is that material variation as well as geometrical variation come into play for the former case. As a result, the in-plane and bending moduli, $A_{ij}$ and $D_{ij}$, are no longer uniform in the repeating region of a hybrid fabric composite.

Figure 2 shows an example of a hybrid fabric composite for $n_g = 8$. The front view is dominated by filling threads and the back side is warp thread dominated. There are two kinds of fiber materials denoted by $\alpha$ and $\beta$, although there is no restrictions regarding the number of thread materials in a hybrid fabric. For the case of Figure 2, the pattern of arrangement of fiber types in the filling direction repeats for every two warp threads. It is defined that $n_{fm} = 2$. In the warp direction, the pattern of arrangement of fiber types repeats for every three filling threads, and $n_{wm} = 3$. The subscript $m$ indicates a material parameter. The following analysis is limited to fabrics containing only two types of fibers densely woven in both directions, i.e. no gaps are allowed.

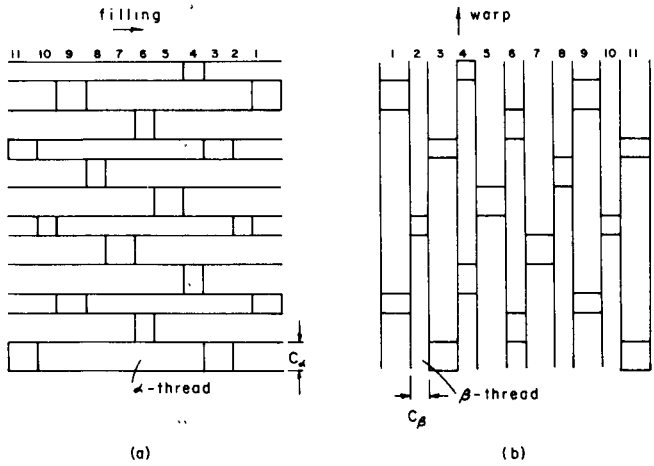


*Figure 2. A hybrid woven fabric with $n_g = 8$, $n_{fm} = 2$ and $n_{wm} = 3$. a) front view, b) back view.*

## DEFINITIONS AND IDEALIZATIONS

It has been adopted that $n_g = n_{fg} = n_{wg}$ specifies the fabric geometrical pattern, and $n_{fm}$ and $n_{wm}$ define the fabric material arrangements. The nota-

tion $n_m$ will be used when the consideration of material parameter is not restricted to any one direction.

In the following the discussions are first focussed on the pattern of hybrid fabrics in one dimension, along the filling or warp direction. The cross-sectional view of a fabric is given in Figure 1e. The fiber yarns of the fabric after resin impregnation and curing with pressure become flattened and more uniformly distributed in the matrix material (Figure 3a). This cross-sectional view of the fabric composite can be idealized by the mosaic model of Figure 3b. With this model a fabric composite can be simply regarded as an assemblage of pieces of asymmetrical cross-ply laminates.

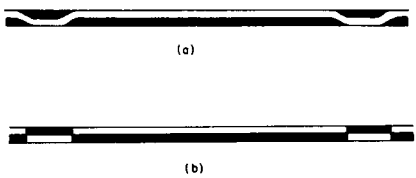


*Figure 3. Cross-sectional views of fabric composites. a) after curing and b) idealized mosaic model.*

If $n_g$ and $n_m$ are prime to each other in a given direction, warp or filling, the pattern of the hybrid fabric will repeat in that direction for every $n_g \times n_m$ threads in the orthogonal direction. For instance, for $n_g = 5$ and $n_{fm} = 3$, Figure 4 shows the pattern of fabric repeats in the filling direction for every 15 warp threads. In general, the pattern of a fabric is repeated in the filling direction after every $n_f$ warp threads, where $n_f$ is the least common multiple ($LCM$) of $n_{fg}$ and $n_{fm}$, or $n_f = LCM\ (n_{fg}, n_{fm})$. Similarly, it is defined $n_w = LCM\ (n_{wg}, n_{wm})$.

Although the size of a basic repeating unit in the filling direction, for instance, is determined by $n_f$, the detail arrangements of fibers may vary. Figure 5 shows two cases of fabric pattern in the filling direction for $n_{fg} = 8$ and $n_{fm} = 2$ ($n_{f\alpha}, n_{f\beta} = 1$) as well as $n_{fg} = 8$ and $n_{fm} = 4$ ($n_{f\alpha} = 3, n_{f\beta} = 1$). Here, $\alpha$ and $\beta$ denote the two types of fiber materials of the hybrid. The notation $\xi$ is used to indicate that the filling thread can be of either $\alpha$ or $\beta$ type. It is obvious from Figure 5 that $n_f = 8$ for both cases and the different repeating patterns are generated by continuously shifting the positions of the warp threads in the filling directions. In general, the number of repeating patterns in the filling direction for a given $n_f$ is equal to the greatest common measure ($GCM$) of $n_{fg}$ and $n_{fm}$ and is denoted by $n_{fi} = GCM\ (n_{fg}, n_{fm})$. Naturally, $n_{fi} = 1$ for the case of Figure 4. Again the notation $n_i$ can be used if the discussion is independent of the direction.

Further comments are necessary for identifying the nature of the interlaced regions of a hybrid fabric. In Figure 5 the interlaced region is "homogeneous" if the threads are identical or "heterogeneous" if the threads are of different types. The notations $HO1^{\alpha}$, $HE3^{\beta}$, etc. are simply for identification purpose pertaining to later discussions. The types of interlacing are termed "mixed" if both homogeneous and heterogeneous interlacing appear in a repeating pattern. This

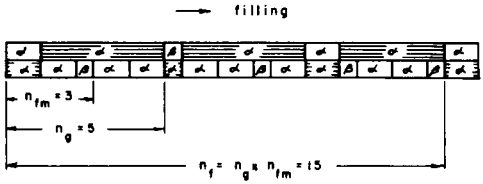


*Figure 4. A fabric where $n_g$ and $n_{fm}$ are prime to each other in the filling direction. α and β denote two types of fibers.*

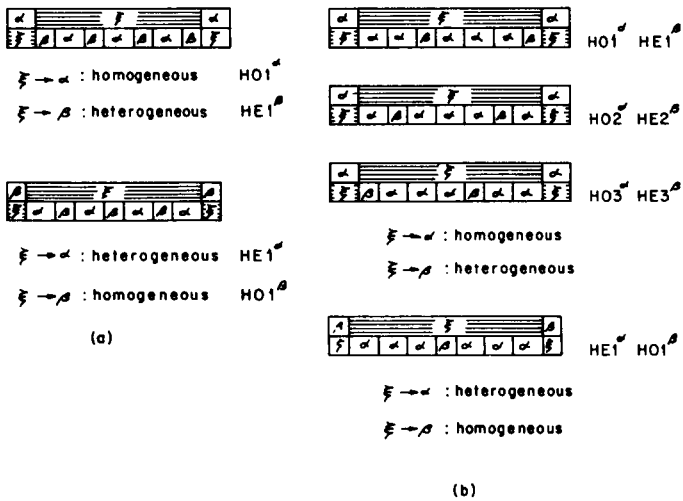


*Figure 5. Homogeneous and heterogeneous interlacings. a) $n_{fg}$ = 8, $n_{fm}$ = 2 ($n^{\alpha}_{fm} = n^{\beta}_{fm} = 1$), b) $n_{fg}$ = 8, $n_{fm}$ = 4 ($n^{\alpha}_{fm} = 3$, $n^{\beta}_{fm} = 1$).*

can occur for $n_g$ and $n_m$ are prime (Figure 4) or non-prime (for instance $n_g$ = 6, $n_{fm}$ = 4) to each other.

Next, identification is made to hybrid fabric patterns in two-dimension based upon the above conclusions established for one-dimensional considerations. Figure 6 shows hybrid fabric patterns for $n_g$ = 8, $n_{fm}$ = 4, and $n_{wm}$ =3 (Figure 6a) and $n_{wm}$ = 4 (Figure 6b). It is noted that, by comparing Figure 6a and Figure 5b, all the interlacing patterns of Figure 5b appear. The area denoted by ABCD in Figure 6a is a possible repeating unit of the fabric. However, there are repetitions in the geometrical and material patterns within this area. It is noted that the patterns of AGIE and IFCH are identical. So are the patterns of GBFI and EIHD. Consequently, the smallest repeating unit of the fabric in two dimensions can be represented by either AGHD or EFCD.

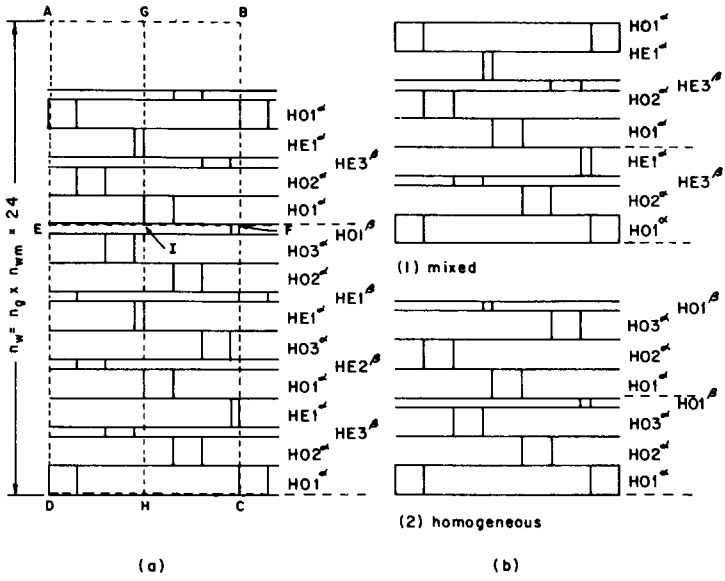


***Figure 6.*** *The two-dimensional basic repeating unit of a hybrid fabric for $n_g$ = 8 and $n_{fm}$ = 4. a) $n_{wm}$ = 3 and $n_g$ and $n_{wm}$ are prime to each other, b) $n_{wm}$ = 4 and $n_g$ and $n_{wm}$ are not prime to each other: (1) mixed interlacing, (2) homogeneous interlacing.*

The area AGHD, for instance, contains 12 ($n_g \times n_{wm}/(n_g/n_{fi})$) filling threads. It can be further concluded that if $n_g$ and $n_m$ are prime to each other in one direction (filling or warp) there exists only one kind of basic repeating unit for defining the two-dimensional fabric. This is true regardless whether $n_g$ and $n_m$ are prime to each other in the other direction.

On the other hand, there exists more than one type of basic repeating unit in two-dimension if $n_g$ and $n_m$ are not prime to each other in both directions. This is illustrated in Figure 6b. In Figure 6b(1) both homogeneous and heterogeneous interlacing in the filling direction occur and the pattern is considered to be "mixed" in two dimensions. The pattern is homogeneous in two-dimenion for Figure 6b(2). There exists two other mixed patterns: [$HO1^{\alpha}$, $HE2^{\beta}$, $HO3^{\alpha}$, $HE1^{\alpha}$] and [$HE1^{\beta}$, $HO2^{\alpha}$, $HO3^{\alpha}$, $HE1^{\alpha}$] and no heterogeneous pattern for the geometrical and material parameters given in Figure 6b.

Let $l_f$ and $l_w$ be the edge lengths of a basic repeating unit in a two-dimensional fabric. If $n_g$ and $n_{wm}$ are prime to each other for the repeating unit AGHD in Figure 6a,

$$\begin{aligned} l_w &= (n^{\alpha}_{wm} C_{\alpha} + n^{\beta}_{wm} C_{\beta}) n_g \\ l_f &= n^{\alpha}_{fm} C_{\alpha} + n^{\beta}_{fm} C_{\beta} \end{aligned} \tag{1}$$

$C_\alpha$ and $C_\beta$ denote thread width as shown in Figure 2. The area of the two-dimensional repeating unit is then given by

$$A_r = n_g(n^\alpha_{wm} C_\alpha + n^\beta_{wm} C_\beta)(n^\alpha_{fm} C_\alpha + n^\beta_{fm} C_\beta)$$

This equation is actually valid for $n_g$ and $n_m$ prime to each other in either filling or warp dirction as well as in both directions. An alternative expression for Eq. (1) can be given by considering the repeating unit of EFCD in Figure 6a,

$$\begin{aligned} l_w &= (n^\alpha_{wm} C_\alpha + n^\beta_{wm} C_\beta) n_{fi} \\ l_f &= (n^\alpha_{fm} C_\alpha + n^\beta_{fm} C_\beta) n_g / n_{fi} \end{aligned} \tag{2}$$

When $n_g$ and $n_m$ are not prime to each other in both directions

$$A_r = \frac{n_w}{n_{wm}}(n^\alpha_{wm} C_\alpha + n^\beta_{wm} C_\beta)(n^\alpha_{fm} C_\alpha + n^\beta_{fm} C_\beta)$$

for $n_w \geqslant n_f$, and

$$A_r = \frac{n_f}{n_{fm}}(n^\alpha_{fm} C_\alpha + n^\beta_{fm} C_\beta)(n^\alpha_{wm} C_\alpha + n^\beta_{wm} C_\beta)$$

for $n_f \geqslant n_w$.

In summary, the pattern of a regular hybrid satin fabric can be determined by the parameters $C_\alpha$, $C_\beta$, $n_g$, $n_m$ and, hence $n_i$, $n_f$ and $n_w$. The "regularity" of fabrics deserves some comments. The concept of regularity is based on the geometrical consideration. Consider, for instance, the regular satin weave of Figure 1d. The geometrical distribution of the interlaced regions in two-dimension can be uniquely determined by two vectors, i.e., (3,1) and (1,3). The vector (3,1) translates an interlaced region by three threads in the filling direction and one thread in warp direction. Other combinations of vectors are also possible, for instance (3,1) and (—2,2) or (2,—2) and (1,3). An example of irregular satin is shown in Figure 1c, where $n_g = 4$ and a set of two vectors cannot be found to generate all the interlaced regions. The term "balanced" hybrid fabric [8] is also used in the paper. In such a fabric, the total number and arrangement of threads of each material in the filling and warp directions are identical. Hence, the relations that $A_{11} = A_{22}$, $D_{11} = D_{22}$ and $B_{11} = -B_{22}$ hold for a balance fabric.

## CONSTITUTIVE EQUATIONS

Based upon the idealizations given in Figure 3, the hybrid fabric composite

can be modelled as an assemblage of pieces of cross-ply laminates. It is further assumed that the shear deformation in the thickness direction is neglected. The constitutive equations are [10—12], for $i,j = 1, 2, 6$

$$\begin{Bmatrix} N_i \\ M_i \end{Bmatrix} = \begin{bmatrix} A_{ij} & B_{ij} \\ B_{ij} & D_{ij} \end{bmatrix} \begin{Bmatrix} \varepsilon_j^0 \\ \kappa_j \end{Bmatrix} \tag{3}$$

or, in the inverted form

$$\begin{Bmatrix} \varepsilon_i^0 \\ \kappa_i \end{Bmatrix} = \begin{bmatrix} a_{ij}^* & b_{ij}^* \\ b_{ij}^* & d_{ij}^* \end{bmatrix} \begin{Bmatrix} N_j \\ M_j \end{Bmatrix} \tag{4}$$

where $N_j$, $M_i$, $\varepsilon_i^0$ and $\kappa_i$ indicate respectively, membrane stress resultants, moment resultants, strain and curvature of the laminate geometrical mid-plane. The definitions of $A_{ij}$, $B_{ij}$, $D_{ij}$, $a_{ij}^*$, $b_{ij}^*$ and $d_{ij}^*$ can be found in [10].

There exists four different types of material combinations in a cross-ply asymmetrical laminate as depicted in Figure 7 where the upper lamina is assumed to be composed of filling threads. In the superscripts used in Figure 7, the first Greek letter identifies the upper layer material and the second letter is for the lower layer. The derivations of the components of $A_{ij}$, $B_{ij}$ and $D_{ij}$ of Eq. (3) for the hybrid fabric composite are straightforward, hence, not given. Also, it is understood that the cross terms $A_{16}$, $A_{26}$, $B_{16}$, $B_{26}$, $D_{16}$ and $D_{26}$ for these asymmetrical cross-ply laminates vanish. Identical approach can be used to derive these constants when the upper lamina is cmposed of warp threads.

## BOUNDS OF STIFFNESS AND COMPLIANCE CONSTANTS

The subject of elastic behavior is basic to the understanding of fabric composites. Kimpara [13] and Hirai and Senba [14] have performed finite element analysis for fabric composites. Ishikawa [9] has recently proposed methods of analysis for obtaining the bounds of elastic moduli in closed forms. The approach of [9] is expanded here to include hybrid composites.

### Iso-Strain

The actual distribution of stress resultant (and moment) and strain (and curvature) over the laminate midplane varies with location in the hybrid fabric composite. As a first approximation, we adopt the assumption of iso-strain in the midplane. Equation (3) is then applied to a fundamental region in the laminate. This region if repeated, should reproduce the geometrical and material arrangements of the entire idealized fabric. It is thus assumed that the behavior of the fundamental region reflects that of the total laminate. The

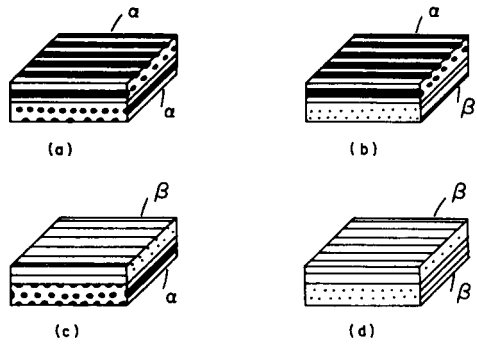


***Figure 7.*** *Material combinations in a cross-ply asymmetrical laminate. The elastic constants for the plies are denoted by a) $A_{ij}^{\alpha\alpha}$, $B_{ij}^{\alpha\alpha}$, $D_{ij}^{\alpha\alpha}$, $a_{ij}^{*\alpha\alpha}$, $b_{ij}^{*\alpha\alpha}$, and $d_{ij}^{*\alpha\alpha}$, b) $A_{ij}^{\alpha\beta}$, $B_{ij}^{\alpha\beta}$, $D_{ij}^{\alpha\beta}$, $a_{ij}^{*\alpha\beta}$, $b_{ij}^{*\alpha\beta}$, and $d_{ij}^{*\alpha\beta}$, c) $A_{ij}^{\beta\alpha}$, $B_{ij}^{\beta\alpha}$, $D_{ij}^{\beta\alpha}$, $a_{ij}^{*\beta\alpha}$, $b_{ij}^{*\beta\alpha}$, and $d_{ij}^{*\beta\alpha}$, and d) $A_{ij}^{\beta\beta}$, $B_{ij}^{\beta\beta}$, $D_{ij}^{\beta\beta}$, $a_{ij}^{*\beta\beta}$, $b_{ij}^{*\beta\beta}$, and $d_{ij}^{*\beta\beta}$.*

dimensions of the fundamental region are denoted by $l_f$ and $l_w$ in the filling and warp directions, respectively. It is also defined that $r = C_\beta/C_\alpha$ (see Figure 2).

$\overline{A}_{ij}$ and $\overline{D}_{ij}$ — The average stress resultant $\overline{N}_1$, for example, is given as an average over the fundamental region in the $x_1\,x_2$ plane

$$\overline{N}_1 = \frac{1}{l_f l_w}\int_0^{l_w}\int_0^{l_f} N_1\,dx_1\,dx_2$$

$$= \frac{1}{l_f l_w}\int_0^{l_w}\int_0^{l_f} [A_{11}^{\xi\eta}\,\varepsilon_1^0 + A_{12}^{\xi\eta}\,\varepsilon_2^0$$

$$+ B_{11}^{\xi\eta}\,\kappa_1 + B_{12}^{\xi\eta}\,\kappa_2]dx_1\,dx_2 \qquad (5)$$

$$= \frac{1}{l_f l_w}\left(\varepsilon_i^0\int_0^{l_w}\int_0^{l_f} A_{1i}^{\xi\eta}\,dx_1\,dx_2\right.$$

$$\left. + \kappa_i\int_0^{l_w}\int_0^{l_f} B_{1i}^{\xi\eta}\,dx_1\,dx_2\right)$$

Where the summation is called for $i = 1, 2, 6$; and $\xi$ and $\eta$ stand for $\alpha$ and $\beta$ phases. From Eq. (5) the following effective stiffness constants of a hybrid fabric composite are defined

$$(\bar{A}_{ij}, \bar{B}_{ij}, \bar{D}_{ij}) = \frac{1}{l_f l_w} \int_0^{l_w} \int_0^{l_f} (A_{ij}^{\xi\eta}, B_{ij}^{\xi\eta}, D_{ij}^{\xi\eta}) dx_1 \, dx_2 \tag{6}$$

These averages, in their simple forms, provide upper bounds of the fabric composite stiffness. If these stiffness constants are inverted, lower bounds of the elastic compliance constants can also be obtained.

Both $A_{ij}^{\xi\eta}$ and $D_{ij}^{\xi\eta}$ for the upper ply are identical to those for the lower ply; general expressions of $\bar{A}_{ij}$ and $\bar{D}_{ij}$ can be written regardless of the relative primeness of $n_g$ and $n_m$. For instance

$$\begin{aligned}\bar{A}_{ij} = {} & \frac{1}{(n_{fm}^{\alpha} + n_{fm}^{\beta} r)(n_{wm}^{\alpha} + n_{wm}^{\beta} r)} [n_{fm}^{\alpha} n_{wm}^{\alpha} A_{ij}^{\alpha\alpha} \\ & + (m_{fm}^{\beta} n_{wm}^{\alpha} A_{ij}^{\alpha\beta} + n_{fm}^{\alpha} n_{wm}^{\beta} A_{ij}^{\beta\alpha}) r \\ & + n_{fm}^{\beta} n_{wm}^{\beta} A_{ij}^{\beta\beta} r^2]\end{aligned} \tag{7}$$

where $n_{fm}^{\alpha}$ and $n_{fm}^{\beta}$ denote the number of $\alpha$ and $\beta$ threads, respectively, within the repeating length of $n_{fm}$ threads in the filling direction. Naturally, $n_{fm}^{\alpha} + n_{fm}^{\beta} = n_{fm}$ and $n_{wm}^{\alpha} + n_{wm}^{\beta} = n_{wm}$. An expression for $\bar{D}_{ij}$ can be obtained if $A_{ij}^{\xi\eta}$ ($\xi, \eta = \alpha, \beta$) in Eq. (7) are replaced by $D_{ij}^{\xi\eta}$. Finally it should be noted that $\bar{A}_{ij}$ and $\bar{D}_{ij}$ can be reduced to the special case of non-hybrid fabric composite of [9]. The upper bounds of $\bar{A}_{ij}$ and $\bar{D}_{ij}$ thus obtained are identical to the $A_{ij}$ and $D_{ij}$ of intermingled hybrids in cross-ply laminate form.

## $\bar{B}_{ij}$

The $\bar{B}_{ij}$ constants can be obtained with the identical approach as in the section $\bar{A}_{ij}$ and $\bar{D}_{ij}$. However, here it is necessary to distinguish the weaving pattern as indicated by $n_g$ *and* $n_m$. Hence, the algebra is more complicated. For $n_g$ and $n_m$ being prime to each other in one direction

$$\begin{aligned}\bar{B}_{ij} = {} & \frac{(n_g - 2)}{n_g} \frac{1}{(n_{fm}^{\alpha} + n_{fm}^{\beta} r)(n_{wm}^{\alpha} + n_{wm}^{\beta} r)} [n_{fm}^{\alpha} n_{wm}^{\alpha} B_{ij}^{\alpha\alpha} \\ & + (n_{fm}^{\beta} n_{wm}^{\alpha} B_{ij}^{\alpha\beta} + n_{fm}^{\alpha} n_{wm}^{\beta} B_{ij}^{\beta\alpha}) r \\ & + n_{fm}^{\beta} n_{wm}^{\beta} B_{ij}^{\beta\beta} r^2]\end{aligned} \tag{8}$$

For $n_g$ and $n_{wm}$ being prime to each other, the result is identical to Eq. (8).

In the case where $n_g$ *and* $n_m$ are not prime to each other in both directions, the expression of $B_{ij}$ depends upon whether the interlacing is homogeneous, heterogeneous or mixed. For instance, for the case of homogeneous interlacing where $n_f \geq n_w$

$$B_{ij} = \frac{1}{n_g(n_{fm}^{\alpha} + n_{fm}^{\beta} r)(n_{wm}^{\alpha} + n_{wm}^{\beta} r)} [(n_g n_{fm}^{\alpha} - 2n_{fi})n_{wm}^{\alpha} B_{ij}^{\alpha\alpha} \\ n_g (n_{fm}^{\beta} n_{wm}^{\alpha} B_{ij}^{\alpha\beta} + n_{fm}^{\alpha} n_{wm}^{\beta} B_{ij}^{\beta\alpha})r \\ + (n_g n_{\mathrm{fm}}^{\beta} - 2n_{fi})n_{wm}^{\beta} B_{ij}^{\beta\beta} r^2] \tag{9}$$

Similar expressions can be derived for heterogeneous interlacing. In the case of mixed interlacing, the expressions depends upon the details of the material arrangement. However, the difference among the $B_{ij}$'s for homogeneous, heterogeneous and mixed interlacing are, in general, not significant within the usual range of $r$, around unity. Therefore Eq. (9) can be used as an approximation of $\bar{B}_{ij}$ for such $r$ values when $n_g$ and $n_m$ are not prime to each other in both directions.

### Iso-Stress

As another method of estimating the bounds of elastic moduli, the assumption of iso-stress is made. Derivations similar to that of Eq. (5) can be performed to obtain the average strain expression of the hybrid fabric composite. The average elastic constants are then given by

$$(\bar{a}_{ij}^{*}, \bar{b}_{ij}^{*}, \bar{d}_{ij}^{*}) = \frac{1}{l_f l_w} \int_0^{l_w} \int_0^{l_f} (a_{ij}^{*\xi\eta}, b_{ij}^{*\xi\eta}, d_{ij}^{*\xi\eta}) dx_1 dx_2 \tag{10}$$

Replacing $A_{ij}^{\xi\eta}$, $B_{ij}^{\xi\eta}$ and $D_{ij}^{\xi\eta}$ in Eqs. (7)—(9) by $a_{ij}^{*\xi\eta}$, $b_{ij}^{*\xi\eta}$ and $d_{ij}^{*\xi\eta}$, explicit expressions of Eq. (10) can be obtained. These are upper bounds of the composite compliance constants, and lower bounds of the stiffness constants when inverted.

## ONE-DIMENSIONAL APPROXIMATION

The approximate solution derived in this section is based upon a combination of the series model of Ishikawa [9] for non-hybrid fabric composites and the mechanics of materials approach of Greszczuk [15] for unidirectional composites. The basic assumptions are that the hybrid fabric composite can be divided into repeating regions in the form of one-dimensional strips, and the equilibrium and compatibility conditions are not exactly satisfied. Figure 8 shows that the hybrid fabric composite is divided into strips along the filling or warp directions. It is then assumed that the resultant stresses ($N_i$) are uniform in each strip.

The division of the strips is made according to the elastic moduli under con-

sideration: along the filling ($x_1$) direction for $A_{11}$, $B_{11}$, $D_{11}$, $a^*_{11}$, $b^*_{11}$ and $d^*_{11}$, along the warp ($x_2$) direction for $A_{22}$, $B_{22}$, $D_{22}$, $a^*_{22}$, $b^*_{22}$ and $d^*_{22}$. Either $x_1$ or $x_2$ directions is admissible for the determination of all the other non-zero constants.

Evidently the average strain in an $\alpha$ thread is different from that of a $\beta$ thread. The one-dimensional average strain can be written, for instance, for the $\alpha$ thread

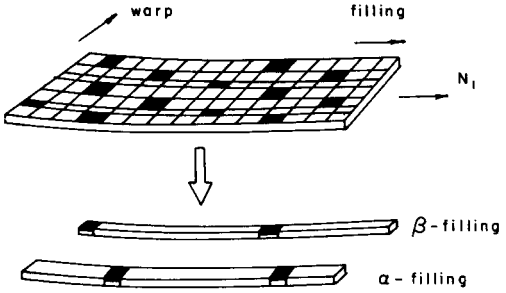


*Figure 8. One dimensional model of the hybrid fabric composite.*

$$\begin{aligned}\bar{\varepsilon}_1^{0\alpha} &= \frac{1}{l_f}\int_0^{l_f} \varepsilon_1^0\, dx_1 \\ &= \frac{1}{l_f}\left(N_i \int_0^{l_f} a_{1i}^{*\xi\eta}\, dx_1 + M_i \int_0^{l_f} b_{1i}^{*\xi\eta} dx_1\right)\end{aligned} \tag{11}$$

where $\xi$ and $\eta$ stand for $\alpha$ and $\beta$. For the case where $n_g$ *and* $n_{fm}$ are prime to each other in the filling direction, the following expressions of averaged compliances are obtained for the $\alpha$-filling threads

$$\begin{aligned}\bar{a}_{ij}^{*\alpha} &= \frac{1}{(n_{fm}^{\alpha} + n_{fm}^{\beta} r)}(n_{fm}^{\alpha} a_{ij}^{*\alpha\alpha} + n_{fm}^{\beta} a_{ij}^{*\alpha\beta} r) \\ \bar{b}_{ij}^{*\alpha} &= \frac{(n_g - 2)}{n_g}\frac{1}{(n_{fm}^{\alpha} + n_{fm}^{\beta} r)}(n_{fm}^{\alpha} b_{ij}^{*\alpha\alpha} + n_{fm}^{\beta} b_{ij}^{*\alpha\beta} r) \\ \bar{d}_{ij}^{*\alpha} &= \frac{1}{(n_{fm}^{\alpha} + n_{fm}^{\beta} r)}(n_{fm}^{\alpha} d_{ij}^{*\alpha\alpha} + n_{fm}^{\beta} d_{ij}^{*\alpha\beta} r)\end{aligned} \tag{12}$$

Naturally expressions of $\bar{A}_{ij}^{\alpha}$, $\bar{B}_{ij}^{\alpha}$ and $\bar{D}_{ij}^{\alpha}$ for the $\alpha$-filling threads can be obtained by inverting $\bar{a}_{ij}^{*\alpha}$, $\bar{b}_{ij}^{*\alpha}$ and $\bar{d}_{ij}^{*\alpha}$ of Eq. (12). Similar procedure can be applied to the $\beta$-filling threads.

Finally, if the average strains in the $\alpha$-threads, $\bar{\varepsilon}_i^{0\alpha}$ and $\bar{\varkappa}_i^{\alpha}$ are not very much different from those in the $\beta$-thread, it is not unreasonable to approximate the entire composite plate with a uniform strain field. Thus the stiffness constants

can be obtained in the sense of volume average. For example,

$$\bar{A}_{11} = \frac{1}{(n^{\alpha}_{wm} + n^{\beta}_{wm} r)} (n^{\alpha}_{wm} \bar{A}^{\alpha}_{11} + n^{\beta}_{wm} \bar{A}^{\beta}_{11} r) \tag{13}$$

For the case of non-hybrid fabrics, namely, $n^{\beta}_{wm} = n^{\beta}_{fm} = 0$, $n^{\alpha}_{wm} = n^{\alpha}_{fm} = 0$ or $r = 0$ or $\infty$, the result of Eq. (13) becomes identical to the lower bound prediction given by Eq. (10).

## NUMERICAL RESULTS

Numerical samples of the above analyses have been performed for the case of graphite/Kevlar fabric in an epoxy matrix. The basic elastic properties of the constituent unidirectional laminae used in this idealized mosaic model are given in Table 1. The fiber volume fraction is chosen to be 65% in order to match that of the experimental systems. Numerical calculations are carried out on a DEC 10 system.

***Table 1. Elastic Properties of the Unidirectional Laminae, $v_f = 65\%$.***

| Material | $E_L$ | $E_T$ | $\nu_L$ | $G_{LT}$ |
|---|---|---|---|---|
| graphite/epoxy [9] | 132 Gpa ($19.3 \times 10^6$ psi) | 9.31 Gpa ($1.36 \times 10^6$ psi) | 0.28 | 4.61 Gpa ($0.67 \times 10^6$ psi) |
| Kevlar/epoxy [8] | 85.3 (12.4) | 5.5 (0.76) | 0.4 | 2.54 (0.37) |

Figure 9 shows the relationship between $A_{11}/h$ and relative fiber volume fraction for "balanced fabrics" [8] where $A_{11} = A_{22}$. The Kevlar and graphite threads are designated as $\beta$ and $\alpha$ threads, respectively. Fabric parameters are so chosen as to coincide with those of [8]: $n_g = 8$, $n_{fm} = 4$ and $n_{wm} = 4$ while $n^{\alpha}_{fm}$, $n^{\beta}_{fm}$, $n^{\alpha}_{wm}$ and $n^{\beta}_{wm}$ vary from 0 to 4. The numbers in the parentheses correspond to values of ($n^{\alpha}_{fm}$, $n^{\beta}_{fm}$, $n^{\alpha}_{wm}$, $n^{\beta}_{wm}$). The ratio of the thread width, $r$, varies from 0 to infinity as the relative fiber volume fraction changes. Since $n_g$ and $n_m$ in this example are not prime to each other, the lower bound predictions are affected by the weaving patterns. Only the lower bound of the case (3,1; 3,1) is shown for the full range of relative fiber volume fraction. Only the homogeneous interlacing types are considered in Figure 9. The upper bounds are identical to one another for these three weaving patterns and are shown by a straight line similar to the rule of mixtures predictions. Solid circles and triangles represent the experimental results of Zweben and Norman [8] for

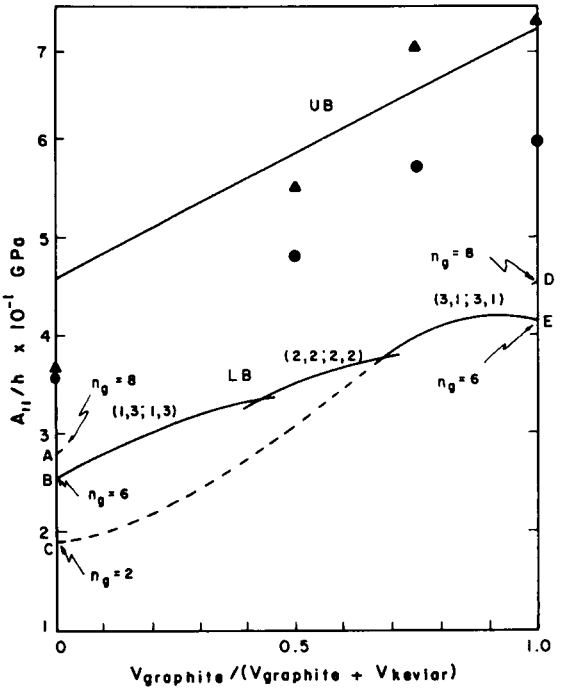


*Figure 9. $A_{11}/h$ vs. relative fiber volume fraction. h denotes specimen thickness. UB: upper bound, LB: lower bound. Experimental results from [8], ●: fabric, ▲: laminate.*

Kevlar/graphite hybrid fabrics and laminates composed of unidirectional laminae of the parent components. The fabrics used in [8] are equivalent to, in our terminology, the categories of (3,1; 3,1) and (2,2; 2,2). The relative thread width is close to $r = 1$ and the interlacing pattern is of the homogeneous type. These results fall in between the bound predictions.

The effect of the fabric geometrical patterns for the parent composites on the bound prediction is worth examining. The Kevlar/epoxy bound prediction is represented in Figure 9 by either $n^{\alpha}_{fm} = n^{\alpha}_{wm} = 0$ or $r = C_{\beta}/C_{\alpha} \to \infty$. Similarly, the graphite/epoxy system corresponds to the case of either $n^{\beta}_{fm} = n^{\beta}_{wm} = 0$ or $r = 0$. The lower bound predictions based on different combinations of $n_g$ and $n_m$ yield different results. Point A in Figure 9 indicates the combination of $n_g = 8$ and $n^{\alpha}_{fm} = n^{\alpha}_{wm} = 0$. Point B is for the limiting case of $n_g = 8$, (1,3; 1,3), and for $r \to \infty$; this case is equivalent to $n_g = 6$ and $n^{\alpha}_{fm} = n^{\alpha}_{wm} = 0$. Point C is obtained from the case of $n_g = 8$, (3,1; 3,1) and $r \to \infty$. The same weaving pattern can be achieved for $n_g = 2$ and $n^{\alpha}_{fm} = 0$. Discussions similar to the above can be made for the case of graphite/epoxy system. Point D is for $n_g = 8$ and $n^{\beta}_{fm} = n^{\beta}_{wm} = 0$. Point E is for $n_g = 8$, (3,1; 3,1) and $r \to 0$; this is equivalent to $n_g = 6$ and $n^{\beta}_{fm} = n^{\beta}_{wm} = 0$. The transition of the geometrical pattern from

$n_g = 8$ to either $n_g = 2$ or 6 as $r$ approaches the limiting values can be understood from Figures 10a and 10b, as well as Eqs. (7) and (9).

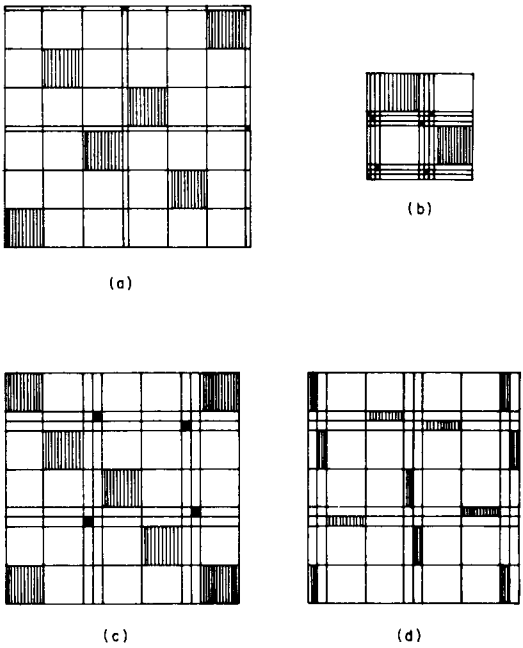


*Figure 10. The transition of fabric geometrical pattern as affected by r. a) $n_g = 8$, (3,1; 3,1) and $r = 1/8$. This pattern becomes $n_g = 6$ as $r \to 0$. b) $n_g = 8$, (3,1; 3,1) and $r = 8$. This pattern becomes $n_g = 2$ as $r \to \infty$. c) homogeneous interlacing for $n_g = 8$, (2,2; 2,2) and $r = 1/4$. This pattern becomes $n_g = 4$ as $r \to 0$. d) heterogeneous interlacing for $n_g = 8$ (2,2; 2,2) and $r = 1/4$. This pattern becomes a cross-ply laminate as $r \to 0$.*

Figure 11 depicts the effect of interlacing types on the lower bound prediction for $n_g = 8$ and (2,2; 2,2). The homogeneous and heterogeneous interlacing types provide considerably different results when $r$ deviates from unity. In the limiting cases of $r = 0$ or $r \to \infty$, the geometrical pattern of the homogeneous fabric is equivalent to that of $n_g = 4$, and the pattern of the heterogeneous fabric tends to that of cross-ply laminates ($n_g \to \infty$). These transitions in geometrical pattern are illustrated in Figures 10c and 10d. The predictions based upon the one-dimensional approximation are also given in Figure 11. When $n_g$ and $n_w$ are prime to each other the lower bound prediction is not affected by the fabric material arrangements as can be seen from Eqs (7)

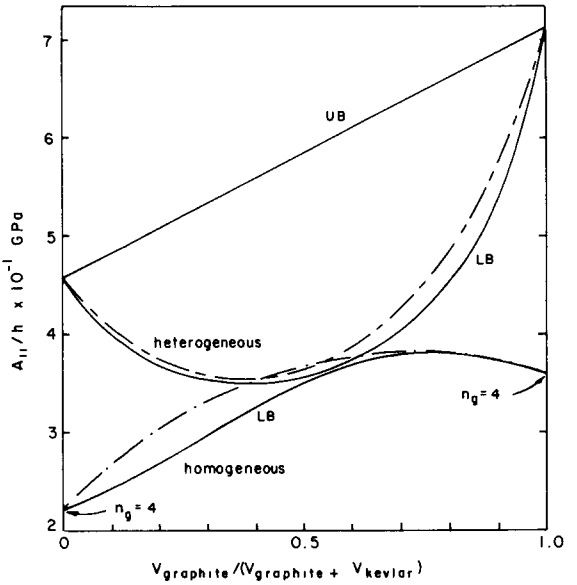


***Figure 11.*** *$A_{11}/h$ vs. relative fiber volume fraction for homogeneous and heterogeneous interlacings. _____: upper and lower bound predictions, - - -; one dimensional approximate solution.*

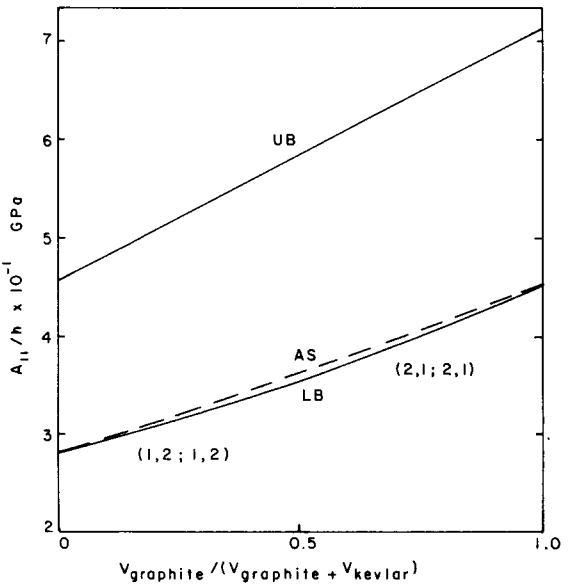


***Figure 12.*** *$A_{11}/h$ vs. relative fiber volume fraction for $n_g$ and $n_m$ being prime to each other. _____: upper and lower bound predictions, - - -: one dimensional approximate solution.*

and (8). Figure 12 demonstrates the case of $n_g = 8$ and $n_{fm} = n_{wm} = 3$ and there is no distinction between the patterns of (2,1; 2,1) and (1,2; 1,2).

Finally, the relationship between $B_{11}/h^2$ and relative fiber volume fraction is demonstrated in Figure 13 for $n_g = 8$ and $n_{fm} = n_{wm} = 4$. Results for both homogeneous and heterogeneous interlacings are shown. In the case of homogeneous interlacing, i.e., (1,3; 1,3), (2,2; 2,2) and (3,1 3,1), the basic trends of the lower bounds are similar to those of Figure 9. However, the upper bound predictions in this case are also affected by the fabric parameters. In the case of heterogeneous interlacing (2,2; 2,2) both the upper and lower bound predictions tend to very large values when $r = 0$ and $r \to \infty$. As a result extremely large couplng effects are realized in these limiting cases.

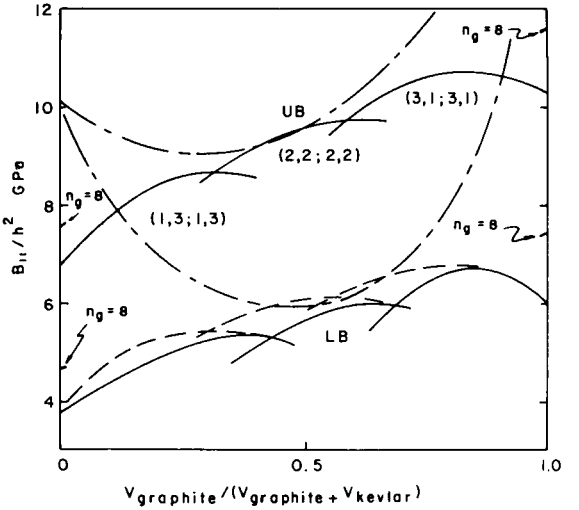


*Figure 13. $B_{11}/h$ vs. relative fiber volume fraction. _____: upper and lower bound predictions for homogeneous interlacing, -.-.-: upper and lower bound predictions for heterogeneous interlacing, and -----: one dimensional approximate solution.*

## CONCLUSIONS

1. The structural characteristics of woven hybrid fabrics have been identified by the material parameter $n_m$ ($n_m$ and $n_{wm}$) as well as the geometrical parameter $n_g$ ($n_{fg}$ and $n_{wg}$). If $n_g$ and $n_m$ of a fabric are prime to each other in one or both directions (filling and warp) there is a unique interlacing pattern. There are more than one type of interlacing pattern of $n_g$ and $n_m$ are not prime to each other in both directions.

2. Analysis of the fabrics is made based upon a mosaic model and the fabric composite can be regarded as an assemblage of asymmetrical cross-ply laminates.

3. Upper and lower bounds of elastic stiffness and compliance of hybrid composites have been obtained based upon the iso-strain and iso-stress assumptions, respectively. The influence of fabric parameters on elastic properties also has been demonstrated. The theory compares very favorably with existing experimental results.

4. The relative primeness of $n_g$ and $n_m$ affect the magnitude of the coupling terms of $B_{ij}$ and $b_{ij}^*$. In the case where $n_g$ and $n_m$ are not prime to each other in both warp and filling directions, the upper and lower bounds of $B_{ij}$ and, hence, the lower bounds of $A_{ij}$ and $D_{ij}$ are influenced by the interlacing types.

5. The transition of $n_g$ from one value to another occurs as the ratio of thread width of the component fibers approaches 0 or $\infty$. In such extreme cases, the magnitude of the coupling terms becomes very large especially for heterogeneous interlacing. The distinct interlacing types for given $n_g$ and $n_m$, however, render nearly identical solutions of bounds when the thread width ratio is around unity.

Essential parameters basic to fabric design have been identified.

## ACKNOWLEDGMENT

This work is supported by the U.S. Army Research Office. The authors also thank Dr. C. Zweben for helpful discussions.

## REFERENCES

1. T. W. Chou and A. Kelly, "Mechanical Properties of Composites," Ann. Rev. Mater. Sci., *10*, 229 (1980).
2. T. W. Chou and M. Gruber, "Elastic Behavior of Hybrid Composites," submitted for publication.
3. M. Gruber, J. Overbeeke, and T. W. Chou, "A Reusable Sandwich Beam for Compression Testing of Fiber Composites," submitted for publication.
4. T. W. Chou and H. Fukuda, "Stiffness and Strength in *Composite Materials; Mechanics, Mechanical Properties and Fabrication,* ed. by K. Kawata and T. Akasaka, The Japan Society for Composite Materials (1981).
5. X. Ji, G. Hsiao and T. W. Chou, "A Dynamic Explanation of the Hybrid Effect," to appear in J. Comp. Mater.
6. E. Miller; *Textiles Properties and Behavior,* (rev. edn.), B. T. Batsford, London, 1976.
7. J. H. Strong; *Foundations of Fabric Structures,* National Trade, 1953.
8. C. Zweben and J. C. Norman, "Kevlar 49/Thornel 300 Hybrid Fabric Composites for Aerospace Applications," SAMPE Quarterly, July 1976, p. 1.
9. T. Ishikawa, "Anti-Symmetric Elastic Properties of Composite Plates of Satin Weave Cloth," Fib. Sci. Tech., Vol. 15 (1981), p. 127.
10. R. M. Jones; *Mechanics of Composite Materials,* Scripta, Washington, D.C., 1975.
11. J. M. Whitney and A. W. Leissa, "Analysis of Heterogeneous Anisotropic Plates," J. Appl. Mech., Vol. 36 (1969), p. 261.
12. S. W. Tsai, "Structural Behavior of Composite Materials," NASA CR-71, 1964.
13. I. Kimpara, private communication.
14. T. Hirai and T. Senba, "On the Mechanical Behavior of Fabric-Strengthtened Composites Considering Three-Dimensional Cross-Linked Structure," ICCM 3, Paris, 1980.
15. L. B. Greszczuk, "Theoretical and Experimental Studies on Properties and Behavior of Filamentary Composites," SPI 21st Conf., Chicago, Illinois (1966), Sect. 8A.